

High pressure diffraction studies on Ca_2RuO_4

P. Steffens,¹ O. Friedt,^{1,2} P. Alireza,³ W. G. Marshall,⁴ W. Schmidt,⁵ F. Nakamura,⁶
S. Nakatsuji,⁷ Y. Maeno,⁷ R. Lengsdorf,¹ M. M. Abd-Elmeguid,¹ and M. Braden¹

¹*II. Physikalisches Institut, Universität zu Köln, Zùlpicher Str. 77, D-50937 Köln, Germany*

²*Laboratoire Léon Brillouin, C.E.A./C.N.R.S., F-91191 Gif-sur-Yvette CEDEX, France*

³*Cavendish Laboratory, University of Cambridge,*

Madingley Road CB3 0HE, Cambridge, United Kingdom

⁴*ISIS Facility, Rutherford Appleton Laboratory, Chilton, Didcot, Oxon OX11 0QX, United Kingdom*

⁵*ILL, 6 Rue Jules Horowitz BP 156, 38042 Grenoble CEDEX 9, France*

⁶*Department of Quantum Matter, ADSM, Hiroshima University, Higashi-Hiroshima 739-8530, Japan*

⁷*Department of Physics, Kyoto University, Kyoto 606-8502, Japan*

(Dated: June 17, 2021, **DRAFT**)

We studied the crystal and magnetic structure of Ca_2RuO_4 by different diffraction techniques under high pressure. The observed first order phase transition at moderate pressure (0.5 GPa) between the insulating phase and the metallic high pressure phase is characterized by a broad region of phase coexistence. The following structural changes are observed as function of pressure: a) a discontinuous change of both the tilt and rotation angle of the RuO_6 -Octahedra at this transition, b) a gradual decrease of the tilt angle in the high pressure phase ($p > 0.5$ GPa) and c) the disappearance of the tilt above 5.5 GPa leading to a higher symmetry structure. By single crystal neutron diffraction at low temperature, the ferromagnetic component of the high pressure phase and a rearrangement of antiferromagnetic order in the low pressure phase was observed.

I. INTRODUCTION.

Among the single-layered ruthenates, different topics have attracted research work during the recent years. A wide variety of physical phenomena occur in these compounds that provide an interesting opportunity for the study of competing ground states and the interplay between structural, magnetic and transport properties. Starting from the well-known unconventional superconductor Sr_2RuO_4 , which possesses the layered perovskite K_2NiF_4 structure, it is only an isovalent substitution of Ca^{2+} by Sr^{2+} that leads to a variety of electronic and magnetic phases^{1,2} and finally to Ca_2RuO_4 – a Mott insulator with antiferromagnetic order ($T_N = 112$ K) at low temperature^{3,4,5,6}.

One of the interesting phenomena that Ca_2RuO_4 displays is a Mott transition to a metallic phase that occurs at $T = 357$ K upon heating under ambient conditions. The insulating Mott phase in Ca_2RuO_4 can also be suppressed by a moderate pressure⁷. At room temperature, Ca_2RuO_4 becomes metallic at about 0.5 GPa. For slightly higher pressure it stays metallic down to lowest temperatures and exhibits ferromagnetic order below $T \simeq 10$ K. The Mott transition in both cases – i.e. as function of temperature and of pressure – coincides with a structural transition. The electronic structure of Ca_2RuO_4 i.e. orbital occupation in its insulating as well as in its metallic phase, is still under debate^{8,9,10,11,12,13}. In view of the crossover from antiferro- to ferromagnetism the pressure dependence of Ca_2RuO_4 is of particular interest, because it provides the possibility to study the interplay between the structure and magnetic degrees of freedom. It is possible that the understanding of the ferromagnetic phase of Ca_2RuO_4 might also be helpful to explain the phenomena in $\text{Ca}_{2-x}\text{Sr}_x\text{RuO}_4$, in which for

$0.2 < x < 0.5$ metamagnetic behaviour and an almost ferromagnetic state near $x = 0.5$ is observed¹⁴. This article, describing the structure solution and direct observation of magnetic ordering by neutron and x-ray diffraction, addresses the current lack of information concerning the nature of the high pressure phase.

II. EXPERIMENTAL.

For the determination of the equation of state, powder samples of Ca_2RuO_4 were studied at the synchrotron beamline F3 at HASYLAB in Hamburg and at the 3T.1 spectrometer at LLB, Saclay. At 3T.1 we used helium gas pressure cells and a constant wavelength $\lambda = 2.38 \text{ \AA}$; the maximum pressure was 0.6 GPa. At F3 diamond anvil cells (Bridgman type, 0.6 mm diameter, pressure medium liquid nitrogen) were used and the lattice constants were calculated from the peak positions in the energy dispersive powder diffraction spectra. The measurement covers the pressure region up to 15 GPa.

For the detailed structural analysis, Rietveld refinable data were collected using the PEARL/HiPr time-of-flight diffractometer at ISIS on a powder sample up to a pressure of almost 10 GPa (Paris-Edinburgh-cell). As the pressure was not measured directly in this setup, the pressure was obtained by a fit of the lattice constants to the equation of state (Fig. 1). All these measurements were done at room temperature.

On two different single crystals, elastic neutron diffraction was measured on the IN12 triple axis spectrometer at the ILL, Grenoble, with a clamp cell. These measurements were performed in (100)-(010) and in (100)-(001) geometry (scattering plane), respectively. They covered the temperature range between 1.5 K and room temper-

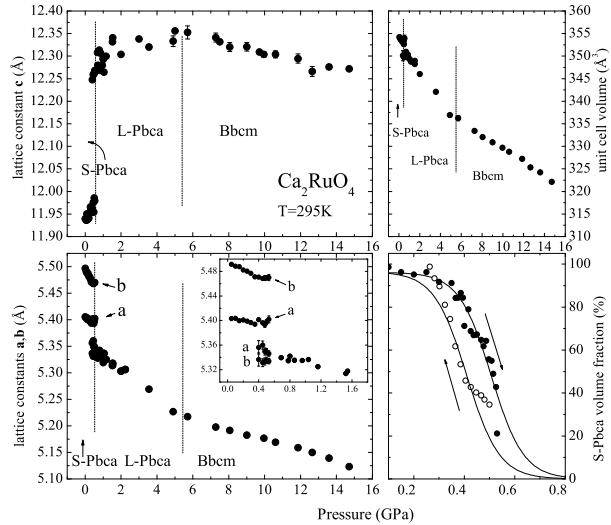


FIG. 1: Left: pressure dependence of the lattice constants of Ca_2RuO_4 . Data were taken by neutron powder diffraction (up to 1 GPa only) and at HASYLAB, Hamburg (whole pressure range). The inset shows a and b near the phase transition from $S\text{-Pbca}$ to $L\text{-Pbca}$. Upper right: evolution of the unit cell volume. Lower right: hysteresis of the $S\text{-Pbca}$ volume fraction at the transition. The corresponding space groups are indicated, the phase transitions are marked by dashed lines.

ature. Crystal sizes in this case were only a few mm^3 – note that up to now large Ca_2RuO_4 single crystals are generally not available because they usually do not withstand the discontinuous structural transition at 357 K. By the use of a triple axis instrument the relatively high background caused by the pressure cell was significantly reduced.

III. RESULTS AND DISCUSSION.

A. Pressure dependence of the crystal structure at room temperature.

As the first step of the structural analysis the pressure dependence of the lattice constants, i. e. the equation of state, was determined up to 15 GPa. The results are shown in Fig. 1. In upstroke, one observes at 0.5 GPa the discontinuous transition from the $S\text{-Pbca}$ into the $L\text{-Pbca}$ phase. Our structural analysis (see below) shows that it is well justified to call these phases (named according to the short, respectively long lattice constant c) exactly like the phases which appear in the phase diagram of $\text{Ca}_{2-x}\text{Sr}_x\text{RuO}_4$ ^{2,5}, because this transition is very similar to the one which occurs in Ca_2RuO_4 upon heating above 357K at ambient pressure. It is of strong first order char-

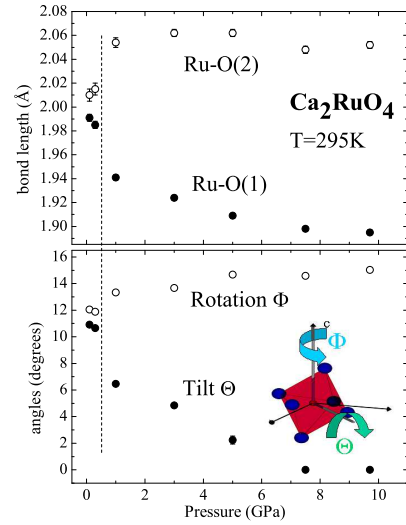


FIG. 2: Top: Evolution of the Ru-O bond lengths. Lower panel: Rotation and tilt angles of the RuO_6 -octahedra. The tilt angle shown is the average of $\text{mit}\Theta(\text{O}2)$ and $\Theta(\text{O}1)$. (Note that the pressure range is smaller than in Figure 1.)

acter and displays a hysteresis of ~ 0.1 GPa (transition around 0.4 GPa in downstroke). At this transition, the lattice volume decreases by about 0.85%, which is slightly more than at the temperature driven transition at ambient pressure². So this transition has to be regarded as just the same transition as the temperature-driven one which is susceptible to pressure because of its negative volume change. Above this first-order transition, the orthorhombic splitting has opposite sign ($a > b$), but the difference is very small and below the limit of detection in the synchrotron spectra; however the PEARL/HiPr neutron diffraction results (see table) yield a splitting $\frac{a-b}{a+b}$ around 10^{-3} . Although it is obvious that pressure stabilizes the state with lower volume, the discontinuous increase of c and the positive $\frac{\partial c}{\partial p}$ over a wide pressure range are remarkable.

The results of the full structure refinement of the data collected at PEARL/HiPr are given in Table I. For the refinement, the programs GSAS¹⁵ and Fullprof¹⁶ were used, and the results checked for consistency. During the refinement, special attention was paid to the determination of the characteristic structural distortions, i. e. the rotation angle of the RuO_6 -octahedra around their vertical axis ($\parallel c$), Φ , and the tilt angle Θ around an axis in the basal plane ($\parallel b$ and parallel to two of the O-O-bonds; for further details see ref. [2]). The results are summarized in Fig. 2.

In the high pressure region, where the tilt distortion is only small, we described the spectra with different structural models, in which a tilt of the octahedra, caused by a nonzero z -position of the O(1)-atom (basal oxygen) and

nonzero x and y of $O(2)$ (apical oxygen), was allowed or forbidden, respectively. It turned out that above 7 GPa there was no significant difference in the R-values, which would justify the lower symmetry. It was also possible to fix the horizontal Ca-positions to zero without affecting the quality of the fit. In contrast, at pressures lower than 5 GPa satisfactory descriptions can only be obtained in the usual $Pbca$ symmetry. At 5 GPa the difference between the two models is only small, but the calculated angles are still significantly above zero.

With respect to Fig. 1, one may argue that the lattice constants a , b and c and as well the cell volume display an anomaly between 5 and 6 GPa: a maximum in c and a kink in a , b and V . Below, the compressibility is $-\frac{1}{V} \frac{\partial V}{\partial p} = 9.0 \cdot 10^{-3} \text{ GPa}^{-1}$, and above, it is only $4.6 \cdot 10^{-3} \text{ GPa}^{-1}$. This behavior is qualitatively very similar to that observed upon heating at ambient pressure, see Fig. 3, where Ca_2RuO_4 undergoes a second transition to a higher symmetric phase at 650 K¹⁷. This analogy allows a relatively precise determination of the pressure at which the phase transition occurs from the data in Fig. 1. We therefore conclude that close to 5.5 GPa the tilt completely vanishes and Ca_2RuO_4 undergoes a continuous phase transition to a phase with space group $Bbcm$ (standard setting $Acam$), which is characterized by a rotation of the RuO_6 -octahedra around the vertical axis only. This is the distortion pattern which is also found in Gd_2CuO_4 ¹⁸. Note that the space group of this phase has to be distinguished from the tetragonal space group $I4_1/acd$, which is found² in $\text{Ca}_{2-x}\text{Sr}_x\text{RuO}_4$ and which is also characterized by the RuO_6 rotation around c , because the sense of the rotation with respect to second nearest neighbor planes is different. (This leads to a twice as long lattice constant c in the case of $I4_1/acd$, $c \simeq 25\text{\AA}$, compared to $Bbcm$ and $Pbca$.) Another difference is that in the orthorhombic space group $Bbcm$ a very small orthorhombicity seems to remain. Due to the absence of the tilt, this reflects the deformation of the octahedron basal plane. The symmetry also allows for a splitting of the in-plane Ru-O bond lengths. Whether this is the case, could not unambiguously be determined²⁴. In contrast to the tilt, the rotational distortion is quite insensitive to pressure; it even increases slightly (Fig. 2).

The uncommon behaviour of the lattice constant c is reflected in the bond length between Ru and $O(2)$, which increases under pressure up to 5 GPa, while the Ru-O(1) bond length decreases continuously. This is obviously correlated to the observed pressure dependence of the resistivity ρ_{ab} and ρ_c (ρ_c increasing, ρ_{ab} decreasing)⁷ – the enhanced overlap of the in-plane orbitals corresponds to the usual effect of pressure and may explain the higher conductivity.

It is tempting to interpret the pressure dependencies of Θ and Φ in view of theoretical calculations that have been carried out on the $\text{Ca}_{2-x}\text{Sr}_x\text{RuO}_4$ phase diagram^{8,9}. In their experiment, Nakamura *et al.*⁷ determined the evolution of the ferromagnetic ordering temperature (partly deduced from resistivity measurements) with pressure. It

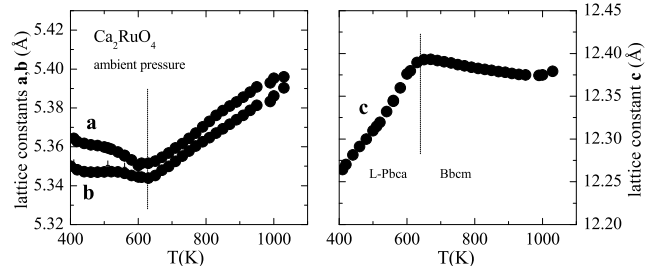


FIG. 3: Temperature dependence of the lattice constants of Ca_2RuO_4 at ambient pressure as measured by x-ray diffraction.

increases from 10 K just above the phase transition to its maximum of 25 K at a pressure ~ 5 GPa, i. e. the increase coincides with the reduction of the tilt angle, and the pressure where the tilt angle finally vanishes is near the maximum of T_C . Fang and Terakura⁹ performed calculations considering the influence of structural distortions on the magnetic properties. They find that the octahedron rotation favors a ferromagnetic ground state due to the smaller bandwidth of Ru d_{xy} , whereas the tilting has the opposite effect. This fits well to the fact that the maximum ordering temperature is at the same pressure where we find the tilt disappearing (at 300K). On the other hand, our structural analysis shows that below 5 GPa there are relatively large tilt angles which obviously do not prevent (ferro-)magnetic order. Near T_C , i. e. at low temperature we even expect the tilt angle to be larger, although there is no structure determination at low temperature in this pressure region yet. The occurrence of ferromagnetism in the tilt distorted structure is also remarkable in view of the fact that in the phase diagram of $\text{Ca}_{2-x}\text{Sr}_x\text{RuO}_4$ it is the octahedron's tilt setting in below a critical Sr-concentration $x=0.5$ which induces antiferromagnetic correlations and drives the system very rapidly away from a ferromagnetic instability^{1,2}.

B. Temperature dependence of the crystal structure under pressure.

The two phase region. The evolution of the lattice constants both of the metallic and of the insulating phase as function of temperature was measured on a single crystal at a constant pressure of approximately 1 GPa. At this pressure, there is a single metallic L - $Pbca$ phase at room temperature, while at low temperatures the crystal partially transforms back into the insulating S - $Pbca$ phase (see inset of Fig. 4), so there is a coexistence of both phases. As shown in Fig. 1, at room temperature the hysteresis as function of pressure is ~ 0.1 GPa, and a coexistence of both phases is found between 0.3 and 0.7 GPa.

At low temperatures this region is broader; in Raman studies by Snow *et al.*¹⁹, the two phase state could be observed up to ~ 1 GPa, and measurements of magnetization and resistivity²⁰ indicate that small amounts of the insulating phase persist even up to ~ 2 GPa. In this region of coexistence the lattice constants of both phases could be measured as function of temperature at about 1 GPa (see Fig. 4).

The insulating phase. In comparison with the low temperature lattice constants of Ca_2RuO_4 at ambient pressure, $a = 5.38 \text{ \AA}$, $b = 5.63 \text{ \AA}$, the lattice is compressed only in b -direction, resulting in a change of shape of the RuO_6 -octahedra; their basal planes are less elongated along b . As mentioned above, Sr-doping has qualitatively the same effect. The origin of the maximum at 150 K is not obvious. Near 150 K, however, is the Néel temperature of the pressurized antiferromagnetic insulating phase (see below).

The metallic phase. More interesting with respect to the discussion of (ferro-)magnetic order are the lattice constants of the metallic phase. We find an unexpected splitting at low temperature²⁶. To determine which type of lattice distortion occurs here, one needs further structural studies.

C. Magnetism in the metallic (high pressure) phase.

Remnant magnetizations in the metallic high pressure phase of Ca_2RuO_4 are of the order of $0.4 \mu_B$ per Ru (with $\mathbf{M} \parallel \mathbf{a}$)^{7,20}. We searched for scattering arising from magnetic ordering in the metallic phase. Bragg scattering caused by ferromagnetic order is located right on the nuclear Bragg reflections; this fact excluded a quantitative determination of the ferromagnetic ordered moment. Nevertheless, the 004-reflection, which has a low nuclear structure factor and offers the best ratio of magnetic to nuclear intensity, displayed a change when heated across the magnetic ordering temperature: with the statistics achievable in our experiment, we obtained a decrease of 1.7 times the uncertainty σ of the integrated intensity between 1.5 and 20 K (at a pressure of ~ 1.5 GPa). Within our experimental accuracy, this is consistent with the value of the remnant magnetization.

We also searched for magnetic order at several other positions in reciprocal space. Among the related ruthenates like $\text{Ca}_{2-x}\text{Sr}_x\text{RuO}_4$ and Ti-doped Sr_2RuO_4 very different magnetic instabilities are found. Ti-doped Sr_2RuO_4 has static incommensurate magnetic order²¹ at a wave vector $(0.7, 0.3, 0)$; paramagnetic $\text{Ca}_{1.5}\text{Sr}_{0.5}\text{RuO}_4$ has a very high susceptibility and displays strongly enhanced magnetic fluctuations²² at $(0.22, 0, 0)$ as well as at the ferromagnetic zone center.

In contrast to macroscopic measurement methods, the direct observation by neutron scattering can give the information whether there are other types of magnetic order than ferromagnetism which fully or partially de-

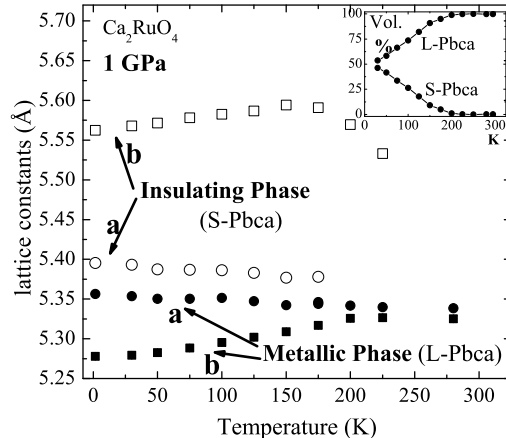


FIG. 4: Temperature dependence of the lattice constants and volume fractions (inset) of both phases at $P=1$ GPa. All data were obtained on heating. In the mixed state, low temperature stabilizes the $S\text{-Pbca}$ phase and the phase transition shifts to higher pressures: at 1 GPa and 1.5 K there is an equal mixture of both phases (inset). Therefore, at low temperature both phases (L - and $S\text{-Pbca}$) could be studied simultaneously and at the same pressure.

termine the observed magnetic properties. However, although measured at several positions in reciprocal space, neither type of incommensurate or antiferromagnetic order could be detected. We estimate that long range order with an ordered moment greater than $\sim 0.25 \mu_B$ would have been detectable.

The exclusion of other scenarios that might appear likely is an additional support that Ca_2RuO_4 really exhibits ferromagnetic order. Other strong arguments⁷ in favor of itinerant ferromagnetism are the size of the macroscopic magnetic moment, which is inconsistent with a possible weak ferromagnetic component accompanying antiferro- or incommensurate magnetic order. The hysteresis is observed in all lattice directions, and the ordering temperatures are one order of magnitude lower than the Néel temperatures in Ca_2RuO_4 . Finally, the temperature dependence of the resistivity indicates 2D itinerant ferromagnetism^{20,23}.

Our examination of magnetic order by elastic neutron scattering supports this scenario of itinerant ferromagnetism as the only one that can account for the magnetic properties of pressurized Ca_2RuO_4 .

D. Magnetism in the insulating (low pressure) phase.

A further result concerns the $S\text{-Pbca}$ phase and its antiferromagnetic order ($T_N=112$ K at $P=0$ GPa). The ordered moment on the Ru sites points along the b -direction of the lattice²⁵. Early studies by neutron pow-

der diffraction⁵ found a mixture of two different antiferromagnetic phases. The alignment of the spin ($M=1.3\mu_B$) is parallel to the b -direction in both cases, but they differ in the stacking sequence of adjacent layers. This leads either to an A-centered or a B-centered magnetic unit cell. The A-centered type of magnetic order ($T_N = 112\text{K}$) was found to be the majority phase at ambient pressure, while the minority B-phase had the higher T_N : $T_N = 150\text{K}$. In some other samples, a similar phase mixture was observed, but in all single crystals of high quality only a single transition at 112 K could be detected²⁰. The appearance of the second phase is most likely caused by small variations in oxygen content – note that Ca_2RuO_4 with excess oxygen was shown to have *only* the B-centered antiferromagnetic order⁵. Samples containing Sr ($\text{Ca}_{2-x}\text{Sr}_x\text{RuO}_4$ with ≥ 0.03) also have only the B-centered order^{2,17} and Néel temperatures of $\sim 150\text{K}$.

At 1 GPa and 1.5 K we were not able to detect any magnetic scattering from the A-centered antiferromagnetic order in the $S\text{-}Pbca$ phase on any of the corresponding Bragg-positions accessible in both crystal orientations. Instead, magnetic scattering was only detectable in the 012-reflection, which originates from magnetic order of the B-centered type. We conclude that there is a single magnetic phase of this type, in contrast to the behavior of the $S\text{-}Pbca$ phase at ambient pressure. We did not determine the full temperature dependence of the magnetic scattering corresponding to the B-type antiferromagnetic order, but at $T \simeq 150\text{K}$ these reflections had entirely disappeared. Susceptibility measurements²⁰ show that T_N is 145 K at $P=0.8\text{GPa}$, i. e. nearly the value which is found in all samples with B-type order at ambient pressure.

The reason for this alteration of the magnetic order from A- to B-type is not obvious, as the coupling between different layers is not yet well understood. However one may argue that this effect is the same as that seen in the Sr-doped samples: very small amounts of Sr – despite the bigger size of the Sr-ion – have a similar effect on the lattice constants and their temperature dependence as the application of pressure¹⁷, so the same subtle structural effect may be the reason for this.

E. The phase diagram.

In Fig. 5 we show a schematic P - T phase diagram of Ca_2RuO_4 which summarizes the results on structure and magnetic order. At ambient pressure, Ca_2RuO_4 is an insulator with an A-centered antiferromagnetic unit cell below $T_N=112\text{K}$. By applying moderate pressure, the magnetic order is changed to B-centered antiferromagnetism. This change occurs at some pressure between 0.2 and 0.8 GPa, and in the case of B-type order the Néel temperature is higher ($T_N>140\text{K}$). Upon increasing temperature or pressure, a first order structural phase transition takes place to the $L\text{-}Pbca$ phase that is metallic and ferromagnetic at low temperature. This phase tran-

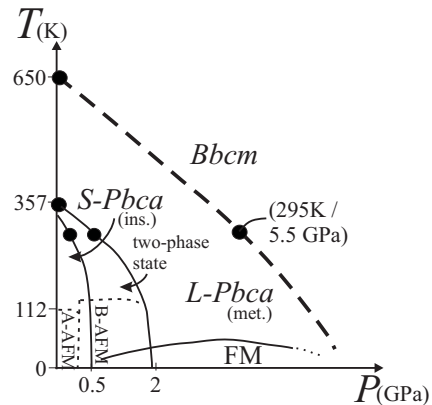


FIG. 5: Schematic structural and magnetic P - T phase diagram of Ca_2RuO_4 (phase boundaries and distances not true to scale). $S\text{-}Pbca$ and $L\text{-}Pbca$ denote the structure with tilt distortion (insulating and metallic respectively) as described in the text, and at the transition a broad region of phase coexistence is found. The phase border to the non-tilted $Bbcm$ structure is known at two points only. A-AFM and B-AFM denote antiferromagnetic order with A- and B-centered magnetic unit cell, respectively. FM is the ferromagnetic metallic phase [7] with maximum T_C around 25 K at 5 GPa.

sition involves a relatively broad region of coexistence of both phases – at low temperature it extends from about 0.5 to 2 GPa; this region is marked as "two-phase-state". At even higher temperatures or pressures, the tilt of the octahedra is completely suppressed; the phase transition to the non-tilted structure with space group $Bbcm$ takes place at 650 K at ambient pressure and at room temperature at 5.5 GPa.

Comparison with the phase diagram of $\text{Ca}_{2-x}\text{Sr}_x\text{RuO}_4$. The application of pressure bears analogy to the effect of a substitution of Ca by Sr. For $0 < x < 0.2$, the Sr-concentration x and the temperature control a first-order transition from an insulating $S\text{-}Pbca$ phase, which is found at low x and low temperature, to a metallic $L\text{-}Pbca$ phase and finally via a second-order phase transition to $Bbcm$ ^{1,2,17}. Antiferromagnetism in the $S\text{-}Pbca$ phase changes from A- to B-centered order upon Sr-doping. For $0 < x < 0.2$, the x - T phase diagram is therefore similar to the P - T phase diagram for pressures below $\sim 2\text{GPa}$, and the crystal structures are basically identical. However, although higher Sr-concentrations finally suppress the tilt down to lowest temperatures, the further evolution is different, because in the $\text{Ca}_{2-x}\text{Sr}_x\text{RuO}_4$ phase diagram the regions $x < 0.2$ and $x > 0.2$ are separated by a first-order phase boundary (due to different rotation schemes, as discussed above in section III A).

IV. CONCLUSION.

We have determined the structural properties of Ca_2RuO_4 up to a pressure of 10 GPa at room temperature and the lattice constants up to 15 GPa. The P - T

phase diagram in Fig. 5 summarizes the results. A first order structural transition leads from the insulating $S\text{-Pbca}$ to the metallic $L\text{-Pbca}$ phase and involves a region in which both phases coexist. In the metallic phase, the tilt angle is strongly reduced, but still significantly different from zero. Only at much higher pressure (above 5.5 GPa at room temperature) the transition into the higher symmetry $Bbcm$ -structure without tilt was observed. In contrast, the rotational distortion is only weakly pressure dependent. In the insulating phase two different types of antiferromagnetic order exist, and pressure seems to control the crossover from A-centered at ambient pressure to B-centered order (with higher Néel temperatures). In the

metallic phase, we observed weak Bragg scattering due to ferromagnetism. The unexpectedly large orthorhombic splitting towards low temperature in this phase indicates further structural effects that have not yet been characterized in detail.

V. ACKNOWLEDGEMENTS.

This work was supported by the Deutsche Forschungsgemeinschaft through SFB 608 and grants from JSPS and MEXT of Japan.

-
- ¹ S. Nakatsuji and Y. Maeno, Phys. Rev. Lett. **84**, 2666 (2000); S. Nakatsuji and Y. Maeno, Phys. Rev. B **62**, 6458 (2000).
- ² O. Friedt, M. Braden, G. André, P. Adelman, S. Nakatsuji and Y. Maeno, Phys. Rev. B **63**, 174432 (2001).
- ³ S. Nakatsuji, S. Ikeda and Y. Maeno, J. Phys. Soc. Jpn. **66**, 1868 (1997).
- ⁴ C. S. Alexander, G. Cao, V. Dobrosavljevic, S. McCall, J. E. Crow, E. Lochner and R. P. Guertin, Phys. Rev. B **60**, R8422 (1999).
- ⁵ M. Braden, G. André, S. Nakatsuji and Y. Maeno, Phys. Rev. B **58**, 847 (1998).
- ⁶ G. Cao, S. McCall, M. Shepard, J.E. Crow and R.P. Guertin, Phys. Rev. B **56**, R2916 (1997).
- ⁷ F. Nakamura, T. Goko, M. Ito, T. Fujita, S. Nakatsuji, H. Fukazawa, Y. Maeno, P. Alireza, D. Forsythe and S. R. Julian, Phys. Rev. B **65**, 220402 (2002).
- ⁸ V. I. Anisimov, I. A. Nekrasov, D. E. Kondakov, T. M. Rice and M. Sigrist, Eur. Phys. J. B **25**, 191 (2002).
- ⁹ Z. Fang and K. Terakura, Phys. Rev. B **64**, 020509(R) (2001); Z. Fang, N. Nagaosa and K. Terakura, Phys. Rev. B **69**, 045116 (2004).
- ¹⁰ T. Hotta and E. Dagotto, Phys. Rev. Lett. **88**, 017201 (2002).
- ¹¹ J. S. Lee, Y. S. Lee, T. W. Noh, S.-J. Oh, Jaejun Yu, S. Nakatsuji, H. Fukazawa, and Y. Maeno, Phys. Rev. Lett. **89**, 257402 (2002).
- ¹² J. H. Jung, Z. Fang, J. P. He, Y. Kaneko, Y. Okimoto, and Y. Tokura, Phys. Rev. Lett. **91**, 056403 (2003).
- ¹³ T. Mizokawa, L. H. Tjeng, G. A. Sawatzki, G. Ghiringhelli, O. Tjernberg, N. B. Brookes, H. Fukazawa, S. Nakatsuji and Y. Maeno, Phys. Rev. Lett. **87**, 077202 (2001); T. Mizokawa, L. H. Tjeng, H.-J. Lin, C. T. Chen, S. Schuppler, S. Nakatsuji, H. Fukazawa, and Y. Maeno, Phys. Rev. B **69**, 132410 (2004).
- ¹⁴ S. Nakatsuji, D. Hall, L. Balicas, Z. Fisk, K. Sugahara, M. Yoshioka and Y. Maeno, Phys. Rev. Lett. **90**, 137202 (2003).
- ¹⁵ A.C. Larson and R.B. von Dreele, Los Alamos National Laboratory Report LAUR 86-748 (2000).
- ¹⁶ J. Rodriguez-Carvajal, Physica B **192**, 55 (1993).
- ¹⁷ P. Steffens *et al.*, to be published.
- ¹⁸ M. Braden, W. Paulus, A. Cousson, P. Vigoureux, G. Heger, A. Goukassov, P. Bourges and D. Petitgrand, Europhys. Lett. **25**, 625 (1994).
- ¹⁹ C. S. Snow, S. L. Cooper, G. Cao, J. E. Crow, H. Fukazawa, S. Nakatsuji and Y. Maeno, Phys. Rev. Lett. **89**, 226401 (2002).
- ²⁰ F. Nakamura *et al.*, to be published.
- ²¹ M. Braden, O. Friedt, Y. Sidis, P. Bourges, M. Minataka and Y. Maeno, Phys. Rev. Lett. **88**, 197002 (2002); M. Minataka and Y. Maeno, Phys. Rev. B **63**, 180504 (2001).
- ²² O. Friedt, P. Steffens, M. Braden, Y. Sidis, S. Nakatsuji and Y. Maeno, Phys. Rev. Lett. **93**, 147404 (2004).
- ²³ M. Hatatani and T. Moriya, J. Phys. Soc. Jpn. **64**, 3434 (1995).
- ²⁴ An unconstrained shift of the O(1) x and y positions can result in two different Ru-O(1) bond lengths. This is an important issue in the discussion of magnetism, because the distortion pattern arising from this could stabilize antiferro-orbital order. Unconstrained refinement yields sizeable splittings up to two percent, but the quality of the fit is *not* affected by enforcing the O(1)-shift to be perpendicular to the bond, i.e. a single Ru-O(1) bond length. The table therefore lists the results of the refinement with equal Ru-O(1) bonds. In the case of the S-Pbca structure at ambient pressure the same question arises – it could be solved by high resolution powder and single crystal studies which did not find significant splitting, see [2,5].
- ²⁵ Note that due to the rotation of the octahedra, the Ru magnetic moment is also slightly canted away from the crystallographic b-axis.
- ²⁶ Here, one has to take account of the possibility, that due to the phase mixture uncontrollable real structure effects influence the results if the domain sizes are very small. However, we consider this as unlikely, as the analysis of the peak widths did not yield any indication for this. In addition, a similar splitting was observed on different samples.

| P (GPa) | 0.1 | 0.3 | 1 | 3 | 5 | 7.5 | 9.7 |
|---------------------------------------|---------------|---------------|---------------|---------------|---------------|-------------|-------------|
| Space group | <i>S-Pbca</i> | <i>S-Pbca</i> | <i>L-Pbca</i> | <i>L-Pbca</i> | <i>L-Pbca</i> | <i>Bbcm</i> | <i>Bbcm</i> |
| a (Å) | 5.4044(6) | 5.4006(5) | 5.3312(6) | 5.2817(6) | 5.2266(9) | 5.2020(6) | 5.1859(6) |
| b (Å) | 5.4904(6) | 5.4760(5) | 5.3160(6) | 5.2689(5) | 5.2187(9) | 5.1865(6) | 5.1673(6) |
| c (Å) | 11.9507(10) | 11.9664(9) | 12.2923(8) | 12.3354(5) | 12.3541(6) | 12.3301(6) | 12.3078(6) |
| R_{wp} (%) | 3.33 | 3.07 | 2.70 | 2.25 | 2.72 | 2.40 | 2.39 |
| Ca x | 0.0108(13) | 0.0092(13) | 0.0116(13) | 0.0109(14) | -0.001(2) | 0 | 0 |
| y | 0.0456(12) | 0.0463(12) | 0.0289(15) | 0.0155(19) | 0.016(2) | 0 | 0 |
| z | 0.3492(5) | 0.3484(5) | 0.3473(4) | 0.3461(3) | 0.3463(3) | 0.3457(3) | 0.3451(3) |
| U_{iso} (Å ²) | 0.0102(15) | 0.0145(17) | 0.0107(11) | 0.0118(10) | 0.0065(11) | 0.0083(8) | 0.0093(8) |
| Ru U_{iso} (Å ²) | 0.0024(10) | 0.0013(8) | 0.0011(7) | 0.0020(6) | 0.0018(8) | 0.0032(7) | 0.0040(8) |
| O(1) x | 0.1953(6) | 0.1966(6) | 0.1909(4) | 0.1894(3) | 0.1847(4) | 0.1851(4) | 0.1832(4) |
| y (=0.5- x) | 0.3030(6) | 0.3019(6) | 0.3094(4) | 0.3110(3) | 0.3155(4) | 0.3153(4) | 0.3173(4) |
| z | 0.0244(4) | 0.0238(4) | 0.0134(4) | 0.0101(4) | 0.0039(10) | 0 | 0 |
| U_{iso} (Å ²) | 0.0082(10) | 0.0080(9) | 0.0077(8) | 0.0070(7) | 0.0058(7) | 0.0071(6) | 0.0070(6) |
| O(2) x | -0.0602(7) | -0.0589(7) | -0.0385(8) | -0.0283(9) | -0.0163(17) | 0 | 0 |
| y | -0.0201(10) | -0.0186(10) | -0.0116(12) | -0.0103(13) | -0.004(2) | 0 | 0 |
| z | 0.1657(4) | 0.1660(4) | 0.1662(3) | 0.1666(2) | 0.1667(3) | 0.1661(2) | 0.1667(2) |
| U_{iso} (Å ²) | 0.0081(11) | 0.0098(11) | 0.0092(10) | 0.0091(8) | 0.0084(8) | 0.0095(6) | 0.0095(6) |
| Ru-O(1) (Å) | 1.991(3) | 1.985(3) | 1.941(2) | 1.924(2) | 1.909(2) | 1.898(2) | 1.895(2) |
| Ru-O(2) (Å) | 2.010(5) | 2.015(5) | 2.054(4) | 2.062(3) | 2.062(3) | 2.048(3) | 2.052(3) |
| O(1)-O(1) $\parallel a$ (Å) | 2.825(5) | 2.818(4) | 2.759(3) | 2.729(3) | 2.703(3) | 2.688(3) | 2.685(3) |
| O(1)-O(1) $\parallel b$ (Å) | 2.808(5) | 2.798(4) | 2.732(3) | 2.711(3) | 2.697(3) | 2.680(3) | 2.675(3) |
| Θ (O1) | 12.0(2) | 11.7(2) | 7.0(2) | 5.3(2) | 2.0(5) | - | - |
| Θ (O2) | 9.83(12) | 9.55(11) | 5.99(12) | 4.4(2) | 2.4(3) | - | - |
| Φ | 12.15(9) | 11.89(9) | 13.33(7) | 13.67(5) | 14.67(6) | 14.59(5) | 15.02(5) |

TABLE I: Results of the room temperature structure refinements of Ca_2RuO_4 under pressure at the PEARL/HiPr beamline (ISIS). Errors of the last digit are given in parentheses and represent only statistical errors, not systematic errors which may for instance arise from correlations between parameters. The position of the Ru-atom is always (0, 0, 0). Anisotropic thermal parameters could not be refined, therefore only the U_{iso} are given.